Systematic study of nuclear β decay

H. Homma, E. Bender,* M. Hirsch,† K. Muto, H. V. Klapdor-Kleingrothaus,‡ and T. Oda
Department of Physics, Tokyo Institute of Technology, Oh-Okayama, Meguro, Tokyo 152, Japan
(Received 29 April 1996)

β-decay properties of nuclei are studied in the framework of proton-neutron quasiparticle random-phase approximation with a schematic Gamow-Teller residual interaction. Particle-hole and particle-particle terms of the separable Gamow-Teller force are consistently included for both β^+ and β^- directions, and their strengths are fixed as smooth functions of mass number A of nuclei in such a way that the calculation reproduces observed β-decay properties of nuclei. Using the fixed interaction strengths, β-decay half-lives of nuclei up to $A=150$ are calculated, and generally good agreement with experiment is obtained. A schematic force which is relevant to the unique first-forbidden decay is also included in a similar way to the Gamow-Teller force, and its effects are studied. [S0556-2813(96)03512-1]

PACS number(s): 23.40.Hc, 21.10.Tg, 21.30.Fe, 21.60.Jz

I. INTRODUCTION

The knowledge of weak interaction rates of nuclei is one of the most important factors for resolving astrophysical problems. Most nuclei of interest in astrophysics are the ones far from stability, and their β-decay properties have to be estimated theoretically.

The most reliable predictions may be obtained by a full diagonalization of an effective Hamiltonian in some model space. Wildenthal [1] obtained nuclear wave functions in the full *sd*-shell model space, which reproduce a wide range of nuclear structure properties. These wave functions are successfully applied to calculate Gamow-Teller β-decay observables [2–4], and are also used in calculations of the electron capture rates in stellar matter [5,6]. Unfortunately, such a sophisticated calculation is tractable only for *sd*-shell nuclei in the current situation, and cannot be applied to *fp*-shell and heavier nuclei which play important roles in the nuclear processes in massive stars. We thus use a simplified model for a systematic study of β-decay properties of a number of nuclei.

Extensive calculations of β-decay rates of nuclei have been performed by several authors previously [7–10]. A calculation based on the gross theory [7] was performed by Takahashi *et al.* more than twenty years ago. This statistical model describes the average properties of the β strength functions, and the shell structure of nuclei is not fully included.

A simple but microscopic model based on the proton-neutron quasiparticle random-phase approximation (pnQRPA) has also been widely used in studies of nuclear β-decay properties. In this model, one first constructs a quasiparticle basis with a pairing interaction, and then solves the RPA equation with a schematic Gamow-Teller (GT) residual interaction. The pnQRPA model was developed by Halbleib and Sorensen [11] by generalizing the usual RPA to describe charge-changing transitions; their original model uses a spherical single-particle model and particle-hole terms of the separable GT force. During about thirty years after the original work of Halbleib and Sorensen, the pnQRPA model has been extended by many authors for its applications to deformed nuclei and nuclei with odd nucleons [12–16].

The extended pnQRPA model has been used to calculate β-decay half-lives of nuclei throughout the nuclidic chart [8–10]. The authors of Refs. [8,9] use particle-hole (ph) terms of the separable GT force for β^- decay [8], whereas for β^+ decay and electron capture [9] they include, in addition to the ph force, particle-particle (pp) force which is known to be important to reproduce the observed suppression of GT strengths in the β^+ direction [17–20]. Their calculations are generally in remarkably good agreement with observed β-decay half-lives. It has been pointed out [21], however, that they fail to reproduce observed systematics of β-decay half-lives [22]. This failure seems to originate from their approach in determining the strengths of the GT force: They fitted the strengths separately for each isotopic chain, and therefore the observed smooth variation of half-lives among neighboring nuclei is not reproduced because the strengths of the GT force are significantly different from one isotopic chain to another.

Recently Möller *et al.* [10] calculated tables of nuclear properties for astrophysical applications, including β-decay half-lives of nuclei ranging from ^{16}O to ^{339}136 and extending from the proton drip line to the neutron drip line. Their calculation is based on the finite-range droplet model and folded-Yukawa single-particle potential, which are used to calculate nuclear ground-state masses and deformations [23]. They calculated GT β-decay rates in the pnQRPA model using only the ph force, the strength of which is a smooth function of mass number.

The pnQRPA model has revealed its usefulness in the description of β-decay properties of nuclei, but at present there are no systematic studies including the ph and pp terms of the GT force consistently for both β^+ and β^- directions. In this paper, we try to determine the strengths of the ph and pp forces such that the calculation reproduces β-decay half-

*Present address: Institut für Theoretische Physik, Universität Tübingen, Auf der Morgenstelle 14, D-72076 Tübingen, Germany.
†Present address: Max-Planck-Institut für Kernphysik, Postfach 103980, D-69029 Heidelberg, Germany.
‡Permanent address: Max-Planck-Institut für Kernphysik, Postfach 103980, D-69029 Heidelberg, Germany.

lives of a wide range of nuclei, assuming the strengths to be smooth functions of mass number A of nuclei. We expect that our approach has an advantage to find out global trends of β-decay properties throughout the periodic system, although specific observables of individual nuclei may not be reproduced well enough. We also examine a possible refinement of the pnQRPA model by introducing a schematic interaction relevant to the unique first-forbidden β decay, which has been totally ignored in the previous QRPA studies, and discuss its effects on the calculated results.

This paper is organized as follows: In Sec. II we briefly describe the method of the calculation. The model has several adjustable parameters as described in Sec. III. They are determined by adjusting the calculated β-decay observables to experimental values. In Sec. IV, β-decay half-lives of nuclei up to $A=150$ are calculated using the fixed parameters, and the accuracy of the calculation is discussed by comparing them with experimental values. Further, effects of the residual interaction which is relevant to the unique first-forbidden decay are discussed.

II. METHOD OF CALCULATION

The probability λ_{fi} of a β transition from an initial nuclear state i to a final nuclear state f can be expressed as

$$\lambda_{fi}=\frac{m_e^5c^4}{2\pi^3\hbar^7}\sum_{\Delta J^\pi} g^2 f(\Delta J^\pi;fi)B(\Delta J^\pi;fi), \tag{1}$$

where $f(\Delta J^\pi;fi)$ and $B(\Delta J^\pi;fi)$ are the integrated Fermi function and the reduced transition probability, respectively, for the transition which induces a spin-parity change ΔJ^π, and g is the weak coupling constant which takes the value g_V or g_A according to whether the ΔJ^π transition is associated with the vector or axial-vector weak interaction. If we are concerned only with allowed transitions, Eq. (1) reduces to

$$\lambda_{fi}=\frac{m_e^5c^4}{2\pi^3\hbar^7}[g_V^2 f(0^+;fi)B(\mathrm{F}_\pm;fi) + g_A^2 f(1^+;fi)B(\mathrm{GT}_\pm;fi)], \tag{2}$$

with the reduced Fermi ($\Delta J^\pi=0^+$) and Gamow-Teller ($\Delta J^\pi=1^+$) transition probabilities for $\beta^\pm$ direction

$$B(\mathrm{F}_\pm;fi)=\frac{1}{2J_i+1}|\langle f||\sum_k t_\pm^k||i\rangle|^2, \tag{3}$$

$$B(\mathrm{GT}_\pm;fi)=\frac{1}{2J_i+1}|\langle f||\sum_k t_\pm^k\sigma^k||i\rangle|^2, \tag{4}$$

where J_i is the total spin of the state i, σ^k and $t_\pm^k$ are the Pauli spin matrix and the isospin raising/lowering operator, which act on the kth nucleon in the nucleus.

The β-decay half-life is readily obtained as

$$T_{1/2}=\frac{\ln 2}{\Sigma_f\lambda_{fi}}, \tag{5}$$

where the sum runs over all states f lying below the initial-state energy.

Since the Fermi transition strength is strongly concentrated in only one final state, i.e., the isobaric analog state (IAS), the reduced transition probability (3) is easily evaluated as

$$B(\mathrm{F}_\pm)=T(T+1)-T_3(T_3\pm 1), \tag{6}$$

where T is the total isospin and T_3 is its projection to the third axis in the initial nuclear state.

As for the Gamow-Teller transitions, the situation is more complicated. The strengths (4) are distributed over a wide range of final states, and so we need to know the structure of the initial and final nuclear states. To do this, we apply the extended pnQRPA model, which we describe briefly in the following. A general description of the model is found in Ref. [15], and a comprehensive representation of the pnQRPA model with separable GT forces is presented in Ref. [16]. We would like the reader to refer to the above materials for details, and will present here only the outline of the calculation.

We start with a deformed Nilsson single-particle model, in which we use a well-known modified oscillator potential with a quadratic deformation. We neglect, as usual, non-vanishing off-diagonal matrix elements between different oscillator major shells. The pairing correlation is taken into account in the BCS approximation using constant pairing forces. The BCS calculation is performed in the deformed Nilsson basis for the proton and neutron systems separately, and then the quasiparticle states are defined by a Bogoliubov transformation. The terms neglected at this stage are much less important than RPA correlations [15].

The ground-state correlation is then introduced by adding a residual interaction to the Hamiltonian, and it is treated in RPA. Creation operators of QRPA phonons are defined as

$$Q_\omega^\dagger(\mu)=\sum_{p,n}[X_\omega^{pn}(\mu)a_p^\dagger a_{\bar{n}}^\dagger - Y_\omega^{pn}(\mu)a_n a_{\bar{p}}], \tag{7}$$

where $a_k^\dagger$ is the creation operator of a quasiparticle in the state k; $k=p,n$ represents the proton and neutron quasiparticle states, and $\bar{k}$ the time-reversed state of k. μ denotes a spherical component of the GT transition operator ($\mu=0,\pm1$), and the sum runs over proton-neutron pairs which satisfy $\mu=m_p-m_n$ and $\pi_p\cdot\pi_n=1$, where m_k and π_k are the spin projection to the symmetric axis and the parity, respectively, of the state k. The excitation energy ω and the amplitudes X_ω, Y_ω of the phonon $Q_\omega^\dagger(\mu)$ are obtained by solving the well-known RPA matrix equation

$$\begin{bmatrix} A & B \\ -B & -A \end{bmatrix}\begin{bmatrix} X \\ Y \end{bmatrix}=\omega\begin{bmatrix} X \\ Y \end{bmatrix}, \tag{8}$$

with [15]

$$A_{pn,p'n'}=\delta_{pn,p'n'}(\epsilon_p+\epsilon_n) + V_{pn,p'n'}^{\mathrm{pp}}(u_pu_nu_{p'}u_{n'}+v_pv_nv_{p'}v_{n'}) + V_{pn,p'n'}^{\mathrm{ph}}(u_pv_nu_{p'}v_{n'}+v_pu_nv_{p'}u_{n'}), \tag{9}$$

$$B_{pn,p'n'} = V^{\rm pp}_{pn,p'n'}(u_p u_n v_{p'} v_{n'} + v_p v_n u_{p'} u_{n'}) - V^{\rm ph}_{pn,p'n'}(u_p v_n v_{p'} u_{n'} + v_p u_n u_{p'} v_{n'}), \quad (10)$$

where ϵ_k is the quasiparticle energy, and v_k/u_k are occupation/unoccupation amplitudes, which are obtained in the BCS calculation.

We use a simple schematic force—so-called GT force—of the form

$$V_{\rm GT} \sim \sum_\mu (-1)^\mu (t_- \sigma_\mu)\cdot(t_+ \sigma_{-\mu}), \quad (11)$$

which has been widely used in studies of GT β-decay properties of nuclei. The GT force (11) has separable ph matrix elements

$$V^{\rm ph}_{pn,p'n'} = +2\chi_{\rm GT} f_{pn}(\mu) f_{p'n'}(\mu), \quad (12)$$

where $\chi_{\rm GT}$ is the strength parameter and f_{pn} is a single-particle GT transition amplitude between Nilsson single-particle states $|p\rangle$ and $|n\rangle$:

$$f_{pn}(\mu) = \langle p|t_-\sigma_\mu|n\rangle. \quad (13)$$

In many previous applications, only the ph terms of the GT force are taken into account, assuming the pp terms to have only a minor effect on GT strength functions [12,13]. However, the pp force is found to be important for describing β^+ and $\beta\beta$ decay [18,19]. We therefore take into account a separable pp force [20], which gives the pp matrix elements

$$V^{\rm pp}_{pn,p'n'} = -2\kappa_{\rm GT} f_{pn}(\mu) f_{p'n'}(\mu). \quad (14)$$

The ph and pp forces are defined to be repulsive and attractive, respectively, when the strength parameters $\chi_{\rm GT}$ and $\kappa_{\rm GT}$ take positive values, reflecting the general feature of the nucleon-nucleon interaction in the $J^\pi = 1^+$ channel. An advantage of using the separable forces is that the RPA matrix equation reduces to an algebraic equation of fourth order [16], which is much easier to solve in comparison with the full diagonalization of the non-Hermitian matrix of a large dimension.

The $J^\pi = 0^+$ ground state of an even-even nucleus is expressed by the QRPA vacuum state $|0^+_{\rm g.s.}\rangle$ defined by $Q_\omega(\mu)|0^+_{\rm g.s.}\rangle = 0$ for all ω and μ. A one-phonon state $|1^+_\omega(\mu)\rangle = Q^\dagger_\omega(\mu)|0^+_{\rm g.s.}\rangle$ then denotes the $J^\pi = 1^+$ excited state of an odd-odd daughter nucleus with the excitation energy $E_{\rm x} = \omega - (\epsilon_p + \epsilon_n)$, where ϵ_p and ϵ_n are energies of the single-quasiparticle states of the smallest quasiparticle energy in the proton and neutron systems, respectively. The reduced transition probability from the ground state $|0^+_{\rm g.s.}\rangle$ to the one-phonon state $|1^+_\omega(\mu)\rangle$ is expressed by

$$B({\rm GT}_\pm) = |\langle 1^+_\omega(\mu)|\sum_k t^k_\pm \sigma^k_\mu |0^+_{\rm g.s.}\rangle|^2. \quad (15)$$

For an odd-mass or odd-odd parent nucleus, the ground state may be expressed as a one-quasiparticle state or a proton-neutron quasiparticle-pair state of the smallest energy. In these cases, quasiparticle transitions are also possible, in addition to the phonon excitations in which the quasiparticle acts merely as a spectator. We introduce phonon correlations to the quasiparticle transitions in first order perturbation [11,13–16]. The explicit descriptions of the probabilities of the phonon excitations and the quasiparticle transitions are presented in Ref. [16].

III. DETERMINATION OF MODEL PARAMETERS

The model briefly described in the preceding section has several adjustable parameters, which should be carefully chosen in order to obtain reliable predictions of β-decay properties of nuclei. In this section, we determine the parameters in such a way that the calculation reproduces observed β-decay properties. Once the parameters are fixed, we can calculate the β transition probabilities (2). We use the constants [24]

$$D \equiv \frac{2\pi^3\hbar^7 \ln 2}{g_V^2 m_e^5 c^4} = 6295 \text{ s} \quad \text{and} \quad \frac{g_A}{g_V} = -1.254, \quad (16)$$

and calculate the Fermi functions for β-decay and electron capture following Refs. [25,26]. Fermi transition probabilities are separately calculated using observed positions of the IAS taken from Ref. [27].

In the following, we discuss the model parameters separately for the two main steps of the QRPA calculation, namely the Nilsson+BCS calculation and the succeeding RPA calculation.

A. Nilsson+BCS calculation: Choice of single-(quasi)particle Hamiltonian

Since the transition rates of nuclei with odd nucleons are determined mainly by quasiparticle transitions, accurate predictions of single-quasiparticle levels are very important. On the other hand, single-particle models have been widely studied concerning various properties of nuclei such as excitation spectra, ground-state masses and deformations, etc. Therefore, we shall determine the single-particle Hamiltonian by using the values of the parameters available in literature.

In the Nilsson calculation, we take the well-known modified oscillator potential [28,29] with the shell-dependent $\boldsymbol{l}\cdot\boldsymbol{s}$- and $\boldsymbol{l}^2$-strength parameters determined by Ragnarsson and Sheline [29]. The oscillator constant is chosen as $\hbar\omega_0 = 45A^{-1/3} - 25A^{-2/3}$ MeV [30]. For simplicity, we consider only quadrupole deformation, which can, in principle, be determined by minimizing the ground state energy. We use, instead of doing this, the ϵ_2 parameters recently published by Möller *et al.* [23]. In order to cover nuclei throughout the periodic system, oscillator major shells $N = 0$–7 are included in the calculation.

In the BCS calculation, we use constant pairing forces. The interaction strengths are fixed to the pairing energy gaps Δ_p and Δ_n for the proton and the neutron systems. The latter may be calculated from mass differences among the neighboring nuclei [31]; alternatively, we may use the global systematics [31]

$$\Delta_p = \Delta_n = 12/\sqrt{A} \text{ MeV}. \quad (17)$$

For a N-nucleon system with N being an odd integer, the BCS equation is usually solved with the even average

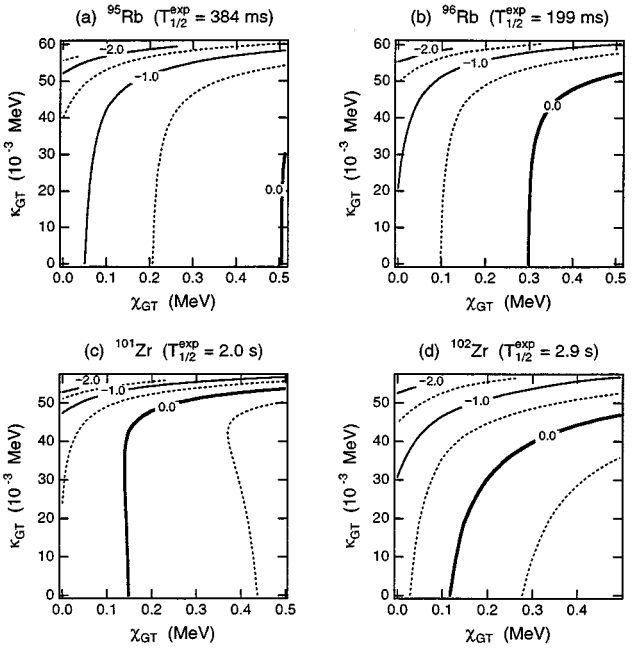

FIG. 1. Contour plots of $\log_{10}(T_{1/2}^{calc}/T_{1/2}^{expt})$ as functions of the strengths of the ph and pp forces.

nucleon number $N-1$, and a N-nucleon state is constructed by putting a quasiparticle upon the ground state of $N-1$ nucleons. In the present calculation, however, we always use N itself for the average nucleon number even if N is odd [32].

In the previous pnQRPA studies [8,9,13], the single-quasiparticle basis is constructed for the parent nucleus. Namely, the parent-nucleus deformation is taken in the Nilsson calculation, and the energy gaps of the parent nucleus are taken in the BCS calculation. Such an approach totally ignores the properties of the daughter nucleus. In addition, the BCS equation is solved under the restriction that the average nucleon number is equal to that of the parent nucleus. Because the resulting quasiparticle levels and occupation amplitudes sometimes depend strongly on this average number, a simple use of the nucleon number of the parent nucleus might be inappropriate.

To reflect the properties of both the parent and daughter nuclei, we construct a kind of averaged nucleus by using the following values for the parameters.

(1) For the deformation, we use the arithmetic mean of the deformation parameters of the parent and daughter nuclei.

(2) For the energy gaps, we use the systematics (17).

(3) For the average nucleon numbers, we use the proton number of the parent nucleus and the neutron number of the daughter nucleus for β^+ decay, and vice versa for β^- decay.

The choice for the average nucleon number is made because the single-quasiparticle level for the decaying nucleon, which is transformed from proton into neutron in β^+ decay and vice versa for β^- decay, is most important.

We have examined various sets of choices for the three model parameters, the deformation, energy gaps, and average nucleon numbers. It has been turned out that the above choices give the overall best fit. Details of the examination will be presented later in this section.

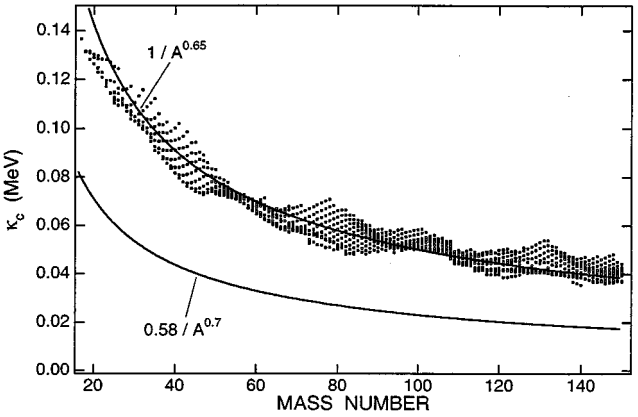

FIG. 2. Critical values κ_c of the strength of the pp force versus mass number. The value of κ_c decreases with increasing mass number A, and is approximately proportional to $1/A^{0.65}$ MeV. In the present work, the strength of the pp force is taken as $\kappa_{GT}=0.58/A^{0.7}$ MeV, which is well below the critical values κ_c.

B. RPA calculation: Strengths of GT residual interaction

The inclusion of the GT residual interaction significantly changes the calculated GT strength distribution, and is of decisive importance for reproducing observed GT strength functions. The strengths of the ph and pp GT forces, which are respectively referred to as χ_{GT} and κ_{GT}, are assumed here to be smooth functions of mass number A of nuclei and are parameterized as

$$\chi_{GT}=\chi_0/A^{\mu}, \tag{18}$$

$$\kappa_{GT}=\kappa_0/A^{\mu}, \tag{19}$$

where χ_0, κ_0, and μ are constants to be determined such that the calculated β-decay properties agree with observation.

In the present work, we focus our attention mainly on β-decay half-lives. First of all, we study how the strengths of the GT forces affect the calculated half-lives. Some typical examples are shown in Fig. 1. As the strength χ_{GT} of the ph force increases, a calculated half-life $T_{1/2}^{cal}$ increases almost linearly because of reduction of the low-lying GT strength. Meanwhile, effects of the pp force depend on whether the parent nucleus has odd nucleons or not [9]: For an even-even parent nucleus, $T_{1/2}^{cal}$ decreases when the strength κ_{GT} increases, with a steeper slope for larger κ_{GT} [see Fig. 1(d)]. On the other hand, $T_{1/2}^{cal}$ is almost constant for small values of κ_{GT} if the parent nucleus has odd nucleons [Figs. 1(a)–(c)], since the β-decay rate of an odd parent nucleus is generally dominated by quasiparticle transitions, which are affected by the pp interaction only through weak correlations with phonons.

In a region of the largest values of κ_{GT}, the half-life $T_{1/2}^{cal}$ decreases suddenly with κ_{GT} in all cases shown in Fig. 1. Because the pp force is attractive, the lowest eigenvalue of the RPA equation approaches zero as the strength κ_{GT} is increased, and finally it becomes imaginary, i.e., the QRPA ''collapses,'' when κ_{GT} exceeds some critical value, say κ_c. Generally the value of κ_c decreases with increasing mass number A, and is expressed approximately as (see Fig. 2)

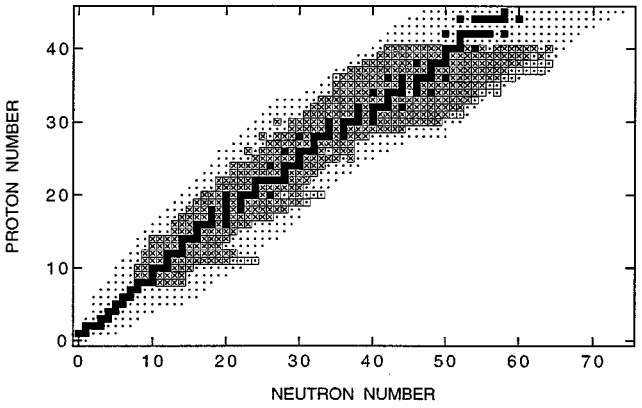

FIG. 3. Nuclei included in the present analysis for determining the strengths of the GT forces. The black squares denote stable isotopes and the dots denote nuclei whose masses are known experimentally [35]. Nuclei which satisfy the selection criteria described in the text are indicated by the open squares (systematics) or crosses (average), according to the choice for the parameters Δ_p and Δ_n.

$$\kappa_c \sim 1/A^{0.65}. \tag{20}$$

We must choose the strength $\kappa_{\rm GT}$ within the physical region, i.e. $\kappa_{\rm GT} < \kappa_c$, for all nuclei.

A method for determining unknown parameters in order that theoretical and observed quantities agree as well as possible is provided by the least-squares-minimization of the model error. We minimize S defined by

$$S = \frac{\sum_{i=1}^{n} w_i \rho_i^2}{\sum_{i=1}^{n} w_i}, \quad \rho_i = \ln(T_{1/2}^{\rm calc}/T_{1/2}^{\rm expt})_i, \tag{21}$$

with respect to the adjustable parameters. Here $T_{1/2}^{\rm expt}$ is the measured half-life and $T_{1/2}^{\rm calc}$ the corresponding calculated quantity for a particular nucleus indicated by the subscript i. Then ρ_i measures the difference between calculated and experimental half-lives of the ith nucleus in the logarithmic scale. Here we use the logarithmic scale because β-decay half-lives vary by many orders of magnitude, and in addition, the calculated and measured half-lives may differ by orders of magnitude.

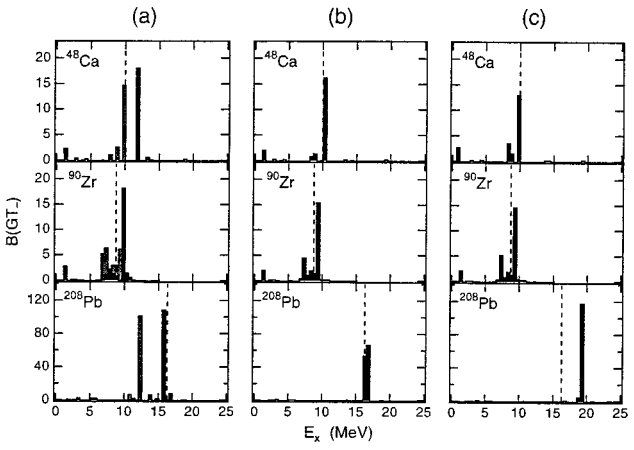

FIG. 4. Calculated β^- strength functions for different choices for the strength of the ph force. The observed positions of the GTGR are indicated by the vertical broken lines. (a) $\chi_{\rm GT} = 23/A$ MeV (solid) and $\chi_{\rm GT} = 15/A$ MeV (shaded). (b) $\chi_{\rm GT} = 5.2/A^{0.7}$ MeV. (c) $\chi_{\rm GT} = 1.3/A^{0.4}$ MeV.

TABLE I. Result of the fit. The strength of the ph force is fixed as $\chi_{\rm GT} = 5.2/A^{0.7}$ MeV. (a) The values of the parameter κ_0 (in MeV) which minimize S of Eq. (21) are presented for several groups of nuclei (see text). The quantities $\overline{r}$ and s measure the accuracy of the calculation and are defined in Eq. (25). (b) The errors of the calculation at $\kappa_0 = 0.58$ MeV.

		(a)			(b)		
Group	n	κ_0 (MeV)	$\overline{r}$	s	κ_0 (MeV)	$\overline{r}$	s
All	373	0.61	1.18	9.37	0.58	1.18	9.37
$T_{1/2}^{\rm expt} < 10^4$ s	309	0.51	1.43	6.03	0.58	1.43	6.04
$T_{1/2}^{\rm expt} < 10^3$ s	269	0.58	1.43	5.25	0.58	1.43	5.25
$T_{1/2}^{\rm expt} < 10^2$ s	228	0.30	1.39	4.13	0.58	1.35	4.15
$T_{1/2}^{\rm expt} < 10^1$ s	159	0.71	1.10	3.10	0.58	1.14	3.11
$T_{1/2}^{\rm expt} < 10^0$ s	88	0.66	0.94	2.40	0.58	0.97	2.40

The quantity $\sqrt{S}$ is the root-mean-square (rms) deviation of ρ_i with the weights w_i. In the simplest definition of the rms deviation, the weights are all taken to be equal. Möller and Nix [33] state that this simplest definition of the rms deviation is unsatisfactory to estimate the model error when the errors associated with the measurements are large, because both the experimental and theoretical errors contribute to the rms deviation. They use statistical arguments and the maximum-likelihood method to decouple the theoretical and experimental errors from each other, and show that, when the uncertainty of the ith measurement is given by $\sigma_{\rm expt}^i$ the theoretical error $\sigma_{\rm calc}$ is estimated by

$$\sigma_{\rm calc}{}^2 = \frac{\sum_{i=1}^{n} w_i^2 (\rho_i^2 - \sigma_{\rm expt}^i{}^2)}{\sum_{i=1}^{n} w_i^2} \tag{22}$$

with

$$w_i = \frac{1}{\sigma_{\rm expt}^i{}^2 + \sigma_{\rm calc}{}^2}, \tag{23}$$

and the best values of the adjustable parameters are obtained by minimizing S of Eq. (21) using the weights w_i defined in

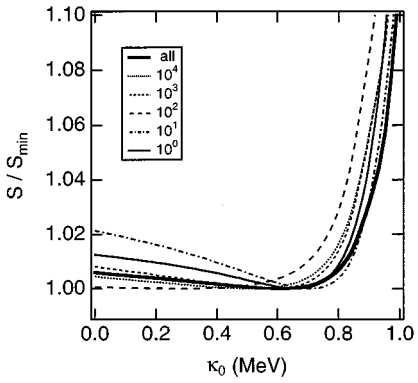

FIG. 5. Dependence of S on κ_0, for the groups presented in Table I.

TABLE II. Agreements between calculated and observed β-decay half-lives evaluated by the quantities defined in Eq. (25), for different choices for the parameters in the Nilsson+BCS calculation described in the text.

Deformation	Energy gap	Nucleon number	n	$\overline{r}$	s
Parent	Parent	Parent	347	1.19	22.4
Parent	Parent	Parent/daughter	355	1.07	15.0
Parent	Average	Parent	347	1.26	15.1
Parent	Average	Parent/daughter	356	1.13	14.6
Parent	Parent/daughter	Parent	365	1.32	21.7
Parent	Parent/daughter	Parent/daughter	370	1.08	15.7
Parent	Systematics	Parent	365	1.13	11.8
Parent	Systematics	Parent/daughter	377	1.13	11.8
Average	Parent	Parent	350	1.27	21.3
Average	Parent	Parent/daughter	352	1.17	13.1
Average	Average	Parent	347	1.32	12.8
Average	Average	Parent/daughter	350	1.17	10.4
Average	Parent/daughter	Parent	368	1.41	19.7
Average	Parent/daughter	Parent/daughter	369	1.21	14.0
Average	Systematics	Parent	371	1.55	20.6
Average	Systematics	Parent/daughter	374	1.18	9.38

Eq. (23). While $\sigma_{\rm calc}$ measures the magnitude of the theoretical error, the systematic trend of the error in the calculation is measured by the mean value of ρ_i,

$$\overline{\rho}=\frac{\Sigma_{i=1}^{n} w_i \rho_i}{\Sigma_{i=1}^{n} w_i}. \tag{24}$$

We use $\sigma_{\rm calc}$ and $\overline{\rho}$ defined above to measure the error of the calculated half-lives, since the experimental errors range from the smallest $\sim 10^{-3}$ to the largest ~ 0.5, where we use relative uncertainty $(\delta T_{1/2}^{\rm expt}/T_{1/2}^{\rm expt})_i$ of the measurement [34] for the experimental error $\sigma_{\rm expt}^{i}$. We also use the following quantities measured in the linear scale:

$$\overline{r}=e^{\overline{\rho}}, \quad s=e^{\sigma_{\rm calc}}. \tag{25}$$

If the calculated half-lives are exactly equal to experimental values, then $\overline{r}=1$ and $s=1$.

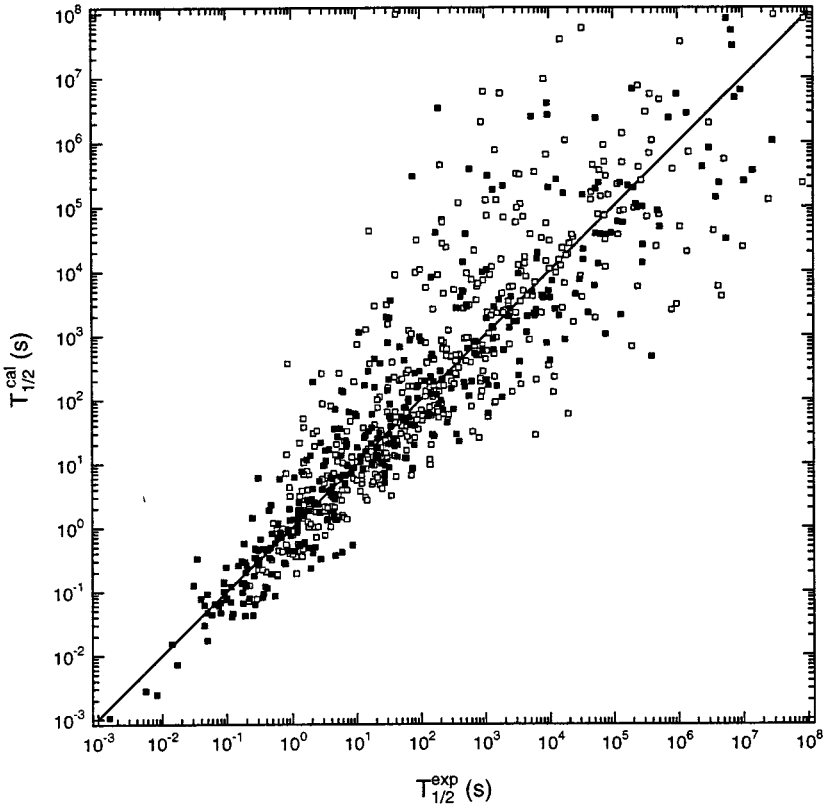

FIG. 6. β-decay half-lives of nuclei with $A \leqslant 150$ calculated by the QRPA model, in comparison with experimental values. The black squares denote nuclei with $Z \leqslant 40$.

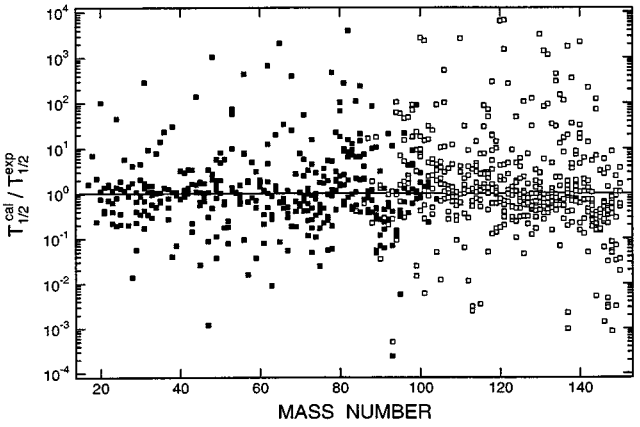

FIG. 7. Same as Fig. 6, but ratios of calculated to experimental half-lives are plotted against mass number.

To fix the parameters by the least-squares-fit, we calculated β-decay half-lives of nuclei which satisfy the following conditions, changing χ_{GT} and κ_{GT} step by step.

(1) Proton number $8 \leqslant Z \leqslant 40$.

(2) The masses needed to calculate the Q_β value are experimentally known [35].

(3) β-decay half-life is experimentally known [34].

The selected nuclei are indicated by the squares in Fig. 3. In the actual analysis in the following, we further exclude some nuclei for which the calculation gives no GT transition within the Q_β window.

We have three adjustable parameters, namely χ_0, κ_0, and μ. We may fix all of these parameters such that the calculated half-lives agree with observation by minimizing S. Then we consider only low-lying GT strengths within the Q_β-window which contribute to the half-life. It is desirable that the calculation gives correct GT strengths also at higher excitation energies.

Information of higher-lying GT strengths is obtained by (p,n) and (n,p) experiments, by which the GT giant resonance (GTGR) is observed at a high excitation energy. Since the calculated position of the GTGR in β^- direction is determined mainly by the ph force [17–20], it is reasonable to fix the strength χ_{GT} such that the observed positions of the GTGR are reproduced. Two values of χ_{GT} determined in this approach have been proposed previously; one is $\chi_{GT}=23/A$ MeV which is derived using the data [36] or ^{208}Pb, and the other is $\chi_{GT}=15/A$ MeV [14] obtained from the Fe region nuclei, both of which assume that χ_{GT} is inversely proportional to mass number A, i.e., $\mu=1$. Figure 4(a) shows GT strength functions for ^{48}Ca, ^{90}Zr, and ^{208}Pb, calculated using the above two values for χ_{GT}. The observed positions of the GTGR are indicated by the broken lines. One can see that the calculated position is too high in ^{48}Ca for the choice $\chi_{GT}=23/A$ MeV and too low in ^{208}Pb for the choice $\chi_{GT}=15/A$ MeV. This suggests a weaker dependence of χ_{GT} on mass number. We calculated the strength functions changing the mass-dependence parameter μ [see Figs. 4(b) and 4(c)], and found that

$$\chi_{GT}=5.2/A^{0.7}\ \text{MeV} \tag{26}$$

well reproduces the positions of the GTGR in all the three cases.

In the present work, we assume the same mass dependences for the ph and pp forces. This assumption seems reasonable, since the $1/A^{0.7}$ dependence determined from observed positions of the GTGR is approximately the same as the mass dependence of the critical values κ_c of the pp force [see Eq. (20) and Fig. 2]. The remaining parameter, κ_0, is determined by minimizing S of Eq. (21). In the calculation of S it is desirable to include as many nuclei as possible. On the other hand, nuclei with long half-lives may cause bad effects on the fit, because the present model is not expected to work well for those nuclei, as will be discussed in the next section. Therefore, we performed the minimization for several groups of nuclei. The results are shown in Table I(a). The first group denoted by ''all'' includes 373 nuclei which are selected in the way described above (see Fig. 3). The other groups include nuclei with half-lives which satisfy the condition in the first column. The values of κ_0 which minimize S differ considerably among the groups, but the change of S in the vicinity of the minimum S_{min} is so gentle, as shown in Fig. 5, and in each case S at $\kappa_0=0.58$ MeV increases no more than 0.5 percent in comparison with the real minimum S_{min} [see also Table I(b)]. So we decided to use

$$\kappa_{GT}=0.58/A^{0.7}\ \text{MeV} \tag{27}$$

for the strength of the pp force. Note that this value of κ_{GT} is well below the critical values κ_c (see Fig. 2).

C. Different choices of the Nilsson+BCS parameters

As has been mentioned before, we use the averaged properties between the parent and daughter nuclei for the parameters in the Nilsson+BCS calculation, namely the deforma-

TABLE III. Accuracy of the present pnQRPA calculation for nuclei with $A \leqslant 150$, evaluated by the quantities defined in Eq. (25). The last three columns show the numbers (percentage) of nuclei for which half-lives are reproduced within factors of 10, 5, and 2, respectively.

Group	n	$\overline{r}$	s	Factor 10	Factor 5	Factor 2
All	842	1.19	18.3	662 (78%)	574 (68%)	339 (40%)
$T_{1/2}^{expt}<10^4$ s	694	1.57	7.69	579 (83%)	510 (73%)	308 (44%)
$T_{1/2}^{expt}<10^3$ s	587	1.52	6.76	506 (86%)	449 (76%)	274 (46%)
$T_{1/2}^{expt}<10^2$ s	446	1.41	5.57	396 (88%)	358 (80%)	222 (49%)
$T_{1/2}^{expt}<10^1$ s	277	1.22	3.60	256 (92%)	230 (83%)	147 (53%)
$T_{1/2}^{expt}<10^0$ s	144	1.02	2.92	111 (97%)	105 (92%)	73 (64%)

TABLE IV. Accuracy of the present pnQRPA calculation for nuclei with $A \leqslant 150$ and $T_{1/2}^{\text{expt}} < 1000$ s. The same quantities as in Table III are separately presented for even-even (e-e), odd mass (odd), and odd-odd (o-o) nuclei.

Group	n	$\overline{r}$	s	Factor 10	Factor 5	Factor 2
All	587	1.52	6.76	506 (86%)	449 (76%)	274 (46%)
e-e	110	1.27	4.78	99 (90%)	93 (84%)	56 (50%)
Odd	296	1.03	4.19	266 (89%)	241 (81%)	183 (48%)
o-o	181	3.18	14.1	141 (77%)	115 (63%)	74 (40%)

tions, the energy gaps, and the average nucleon numbers. To check the validity of this choice, we compare agreement between calculated and experimental half-lives for several choices for these parameters. The examined choices here are summarized as follows.

(1) Deformations: (a) parent; (b) average.

(2) Energy gaps: (a) parent; (b) average; (c) parent/daughter; (d) systematics.

(3) Average nucleon numbers: (a) parent; (b) parent/daughter.

Here ''parent'' is the value in the parent nucleus, and ''average'' is the mean value of the parent and daughter nuclei. In the case ''parent/daughter'' for the energy gaps and the nucleon numbers, we use the value in the parent (daughter) nucleus for the proton (neutron) system for β^+ decay, and vice versa for β^- decay. This is not examined for the deformations, since the proton and neutron states are expressed by different sets of basis wave functions if we use different deformation parameters for the proton and neutron systems. Finally, ''systematics'' means that we use the systematics (17) for the energy gaps; otherwise we calculate them using observed masses [35] of neighboring nuclei.

Table II shows the agreement between the calculated and observed half-lives analyzed by use of the quantities defined in Eq. (25). In the analysis we include nuclei selected in the same way as in the determination of the strengths of the GT forces (see Fig. 3). Note that we have an additional condition if the energy gaps are calculated from masses of neighboring nuclei; we need their experimental values. The nuclei which satisfy all conditions in those cases are indicated by the crosses in Fig. 3.

One can see from Table II that the mean $\overline{r}$ is close to unity in all cases. On the other hand, the values of s differ considerably among different parameter sets, and in general, better descriptions of β-decay half-lives are obtained by use of averaged properties of the parent and daughter nuclei. This indicates that the single-quasiparticle basis should be constructed for a kind of averaged nucleus, not for the parent nucleus, in order to obtain accurate predictions of β-decay properties. In fact, our choice (the bottom row in Table II) gives the smallest s.

IV. CALCULATION OF β-DECAY HALF-LIVES INCLUDING HEAVIER NUCLEI

We have calculated β-decay half-lives of nuclei with mass number $A \leqslant 150$ using the parameters of the separable Gamow-Teller forces determined in the preceding section [Eqs. (26) and (27)]. In this section, we discuss the accuracy of the present calculation by comparing the calculated and experimental half-lives. We also discuss a possibility to improve the pnQRPA model by including the effects of forbidden transitions.

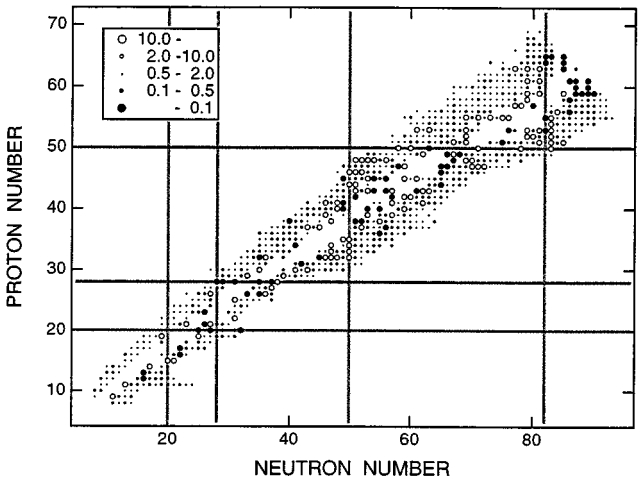

FIG. 8. Agreement between calculated and observed half-lives. The ratios of calculated to experimental half-lives are distinguished by different markers.

A. Comparison with experiment

We illustrate in Figs. 6 and 7 the agreement between the calculated and observed half-lives. Figure 6 shows that the calculation reproduces general trend of β-decay half-lives. The scatter of the points in the figure around the line $T_{1/2}^{\text{calc}} = T_{1/2}^{\text{expt}}$ increases as $T_{1/2}^{\text{expt}}$ increases. This can be understood by the following considerations: First, some nuclei with long half-lives are expected to be dominated by forbidden decay, which we have not considered in the present calculation. Second, a longer half-life generally corresponds to a smaller Q_β value, hence errors in the calculated GT strength have larger effect upon the calculated half-life.

We have fixed the strength of the pp force by adjusting the calculated β-decay half-lives to observed values for nuclei with proton number $Z \leqslant 40$, which are indicated by the black squares in Figs. 6 and 7. The figures also include heavier nuclei indicated by the open squares. For the latter nuclei, no significant change is found in the quality of agreement. This seems to justify the $1/A^{0.7}$ dependence of the GT forces and indicates the validity of the strength parameters of the GT forces in the predictions of β-decay properties of heavier nuclei.

A more quantitative analysis can be made with the help of the quantities defined by Eq. (25). Table III lists the same quantities as in Table I for nuclei with $A \leqslant 150$. The error of the calculation is slightly larger compared to the result in Table I, which includes only nuclei with $Z \leqslant 40$, but the general features are unchanged. The table also shows the numbers of nuclei whose half-lives are reproduced within factors of 10, 5, and 2. For example, the present calculation reproduces 97% of experimentally known half-lives shorter than 1 s within a factor of 10. In Table IV we select nuclei with $T_{1/2}^{\text{expt}} < 1000$ s and show the results separately for even-even, odd-odd, and odd-mass nuclei. It is seen that the calculation tends to overestimate half-lives for odd-odd nuclei, while $\overline{r}$ is

TABLE V. Number of pairs of nuclei which violate the semi-empirical inequalities (28a)–(28h) for experimental and calculated half-lives. T and T' represent the lhs and rhs of the inequality, respectively. All the inequalities (28) require $T>T'$.

Inequality	Total number of tested pairs	Number of violation (expt)			Number of violation (calc)		
		$T\gg T'$	$2T\gg T'$	$3T\gg T'$	$T\gg T'$	$2T\gg T'$	$3T\gg T'$
a	131	2	1	0	3	2	2
b	157	5	2	2	38	14	6
c	101	3	2	1	3	2	2
d	140	1	0	0	7	5	2
e	130	1	1	0	0	0	0
f	145	1	0	0	0	0	0
g	126	1	1	1	0	0	0
h	164	1	0	0	10	3	1

closer to unity in even-even and odd-mass cases. This trend is seen also in the previous pnQRPA calculations [9,13] (see TABLE E of Ref. [9]).

The accuracy of the calculation for each nucleus included in the present analysis is shown graphically in Fig. 8. Generally, the calculation is inaccurate for nuclei near the β-stability line, and also for those which have the proton or neutron number near the magic numbers. For some of those nuclei the calculated half-lives are significantly improved by considering forbidden transitions, as will be shown later.

Another test of the model calculation is provided by the semi-empirical inequalities for β-decay half-lives given by Kondoh and Yamada [22]:

$$T^{-}_{1/2}(Z,2n)>T^{-}_{1/2}(Z,2n+2), \tag{28a}$$

$$T^{-}_{1/2}(Z,2n)>T^{-}_{1/2}(Z,2n+1), \tag{28b}$$

$$T^{-}_{1/2}(2m,N)>T^{-}_{1/2}(2m-2,N), \tag{28c}$$

$$T^{-}_{1/2}(2m,N)>T^{-}_{1/2}(2m-1,N), \tag{28d}$$

$$T^{+}_{1/2}(2m,N)>T^{+}_{1/2}(2m+2,N), \tag{28e}$$

$$T^{+}_{1/2}(2m,N)>T^{+}_{1/2}(2m+1,N), \tag{28f}$$

$$T^{+}_{1/2}(Z,2n)>T^{+}_{1/2}(Z,2n-2), \tag{28g}$$

$$T^{+}_{1/2}(Z,2n)>T^{+}_{1/2}(Z,2n-1), \tag{28h}$$

where m and n are arbitrary integers and $T^{\pm}_{1/2}(Z,N)$ denotes $\beta^{\pm}$-decay half-life of the nucleus with Z protons and N neutrons. These inequalities are quite well satisfied by observed half-lives, as shown in Table V. For the calculation the num-

TABLE VI. Accuracy of the calculated β-decay half-lives evaluated by the average deviation $\overline{x}$ defined in Eq. (29). (a) Present calculation. (b) The pnQRPA calculation by Staudt *et al.* [8] and Hirsch *et al.* [9].

(a) Present calculation

		β^- decay			β^+/EC decay		
	Group	N	n	$\overline{x}$	N	n	$\overline{x}$
$x_i\leqslant 10$	$T^{\rm expt}_{1/2}<10^6$ s	390	299 (76.7%)	3.00	408	351 (86.0%)	2.56
	$T^{\rm expt}_{1/2}<60$ s	250	218 (87.2%)	2.81	158	148 (93.7%)	2.12
	$T^{\rm expt}_{1/2}<1$ s	69	66 (95.7%)	2.64	45	45 (100.0%)	1.67
$x_i\leqslant 2$	$T^{\rm expt}_{1/2}<10^6$ s	390	132 (33.8%)	1.43	408	203 (49.8%)	1.41
	$T^{\rm expt}_{1/2}<60$ s	250	105 (42.0%)	1.41	158	101 (63.9%)	1.37
	$T^{\rm expt}_{1/2}<1$ s	69	35 (50.7%)	1.43	45	38 (84.4%)	1.35

(b) References [8,9]

		β^- decay [8]			β^+/EC decay [9]		
	Group	N	n	$\overline{x}$	N	n	$\overline{x}$
$x_i\leqslant 10$	$T^{\rm expt}_{1/2}<10^6$ s	654	472 (72.2%)	1.85	894	706 (79.0%)	2.06
	$T^{\rm expt}_{1/2}<60$ s	325	313 (96.3%)	1.67	327	304 (93.0%)	1.72
	$T^{\rm expt}_{1/2}<1$ s	106	105 (99.1%)	1.44	81	78 (96.3%)	1.85
$x_i\leqslant 2$	$T^{\rm expt}_{1/2}<10^6$ s	654	369 (56.4%)	1.37	894	489 (54.7%)	1.36
	$T^{\rm expt}_{1/2}<60$ s	325	267 (82.2%)	1.36	327	245 (74.9%)	1.31
	$T^{\rm expt}_{1/2}<1$ s	106	96 (90.6%)	1.35	81	59 (72.8%)	1.23

TABLE VII. Accuracy of the calculated β-decay half-lives evaluated by the quantities defined in Eqs. (31) and (32). (a) Present calculation. (b) The pnQRPA calculation by Möller *et al.* [10].

(a) Present calculation

Group		β^- decay n	$M^{10}_{r_1}$	$\sigma^{10}_{r_1}$	β^+/EC decay n	$M^{10}_{r_1}$	$\sigma^{10}_{r_1}$
$T^{\text{expt}}_{1/2}<1$ s	e-e	10	1.15	2.36	5	0.95	1.26
	Odd	31	0.60	2.24	24	1.06	2.06
	o-o	28	1.75	4.96	16	1.03	1.40
$T^{\text{expt}}_{1/2}<10$ s	e-e	34	1.01	2.93	13	1.14	1.85
	Odd	81	0.92	3.84	47	0.98	1.98
	o-o	66	1.89	4.60	36	1.79	3.59
$T^{\text{expt}}_{1/2}<100$ s	e-e	52	1.13	3.58	26	1.00	2.27
	Odd	127	1.07	4.29	94	0.89	2.28
	o-o	85	3.15	10.51	62	2.37	7.54
$T^{\text{expt}}_{1/2}<1000$ s	e-e	63	1.39	6.10	47	1.11	3.03
	Odd	157	1.10	5.55	139	0.97	2.78
	o-o	93	3.02	10.25	88	3.36	11.30

(b) Möller *et al.* [10]

Group		β^- decay n	$M^{10}_{r_1}$	$\sigma^{10}_{r_1}$	β^+/EC decay n	$M^{10}_{r_1}$	$\sigma^{10}_{r_1}$
$T^{\text{expt}}_{1/2}<1$ s	e-e	10	3.84	3.08	9	3.52	2.03
	Odd	35	0.59	2.64	30	1.79	3.97
	o-o	29	0.59	2.91	21	1.49	3.99
$T^{\text{expt}}_{1/2}<10$ s	e-e	34	2.50	4.13	33	1.62	4.46
	Odd	85	0.78	4.81	77	1.07	3.38
	o-o	59	0.76	8.83	43	1.22	5.77
$T^{\text{expt}}_{1/2}<100$ s	e-e	54	2.61	4.75	63	0.98	3.52
	Odd	133	1.11	9.45	149	0.73	3.33
	o-o	88	2.33	49.19	85	1.30	11.37
$T^{\text{expt}}_{1/2}<1000$ s	e-e	71	6.86	58.48	101	0.83	3.16
	Odd	194	2.77	71.50	238	0.63	4.47
	o-o	115	3.50	72.02	146	1.37	17.49

ber of violation is larger compared to that for the observed half-lives, but in most cases the violation is small; as is seen in the table, there are only a few pairs which violate the inequalities by more than a factor of 3.

The present calculation satisfies the inequalities (28a)–(28h) much better than the quite similar pnQRPA calculations [8,9], especially those between nuclei with different proton number (inequalities c, d, e, and f) [21]. In Refs. [8,9] the strengths of the GT forces are fixed separately for each isotopic chain, hence the origin of the violation is probably large differences of the strengths between nuclei in both sides of the inequalities. In the present calculation we are free from this kind of problem, since the strength parameters are assumed to be smooth functions of mass number and thus take similar values for nuclei in both sides of the inequalities.

B. Comparison with previous QRPA calculations

Extensive pnQRPA calculations of β-decay half-lives have been done by two groups [8–10]. The authors of Refs. [8,9] use the ph terms of the GT force for β^- decay, and both the ph and pp forces for β^+ decay and electron capture. The strengths of the ph and pp forces are fitted to experimental half-lives of known isotopes with a fixed atomic number. They evaluate the accuracy of their calculated half-lives by the average deviation $\overline{x}$ defined by

$$\overline{x}=\frac{1}{n}\sum_{i=1}^{n} x_i\,, \tag{29}$$

where

TABLE VIII. The accuracy of the calculated β-decay half-lives evaluated by the quantities defined in Eqs. (31) and (32). (a) Nuclei with $Z \leqslant 40$, which are included in the fit of the strengths of the GT forces. (b) Nuclei with $Z > 40$, which are not included in the fit.

(a) $Z \leqslant 40$

Group		β^- decay n	$M_{r_1}^{10}$	$\sigma_{r_1}^{10}$	β^+/EC decay n	$M_{r_1}^{10}$	$\sigma_{r_1}^{10}$
$T_{1/2}^{\rm expt} < 1$ s	e-e	7	0.91	2.19	5	0.95	1.26
	Odd	21	0.59	2.29	24	1.06	2.06
	o-o	17	1.54	3.44	14	1.03	1.34
$T_{1/2}^{\rm expt} < 10$ s	e-e	20	1.08	3.22	9	1.26	1.91
	Odd	48	0.83	3.59	32	1.06	1.89
	o-o	33	1.85	4.02	18	1.14	2.08
$T_{1/2}^{\rm expt} < 100$ s	e-e	29	1.36	4.19	11	1.19	1.87
	Odd	75	1.13	4.09	47	0.92	1.98
	o-o	44	2.35	4.35	23	1.79	7.60
$T_{1/2}^{\rm expt} < 1000$ s	e-e	33	1.89	8.35	14	1.15	1.79
	Odd	91	1.15	4.93	57	0.93	2.61
	o-o	48	2.31	4.25	27	2.25	9.86

(b) $Z > 40$

Group		β^- decay n	$M_{r_1}^{10}$	$\sigma_{r_1}^{10}$	β^+/EC decay n	$M_{r_1}^{10}$	$\sigma_{r_1}^{10}$
$T_{1/2}^{\rm expt} < 1$ s	e-e	3	2.00	2.17	0		
	Odd	10	0.61	2.14	0		
	o-o	11	2.13	7.59	2	1.02	1.69
$T_{1/2}^{\rm expt} < 10$ s	e-e	14	0.91	2.49	4	0.92	1.60
	Odd	33	1.07	4.15	15	0.82	2.09
	o-o	33	1.93	5.21	18	2.83	4.57
$T_{1/2}^{\rm expt} < 100$ s	e-e	23	0.90	2.70	15	0.88	2.50
	Odd	52	0.99	4.56	47	0.86	2.57
	o-o	41	4.33	19.96	39	2.80	7.37
$T_{1/2}^{\rm expt} < 1000$ s	e-e	30	0.99	3.67	33	1.09	3.55
	Odd	66	1.04	6.45	82	0.99	2.89
	o-o	45	4.03	19.43	61	4.02	11.72

$$x_i = \begin{cases} T_{1/2}^{\rm expt}/T_{1/2}^{\rm calc} & \text{if} \quad T_{1/2}^{\rm expt} \geqslant T_{1/2}^{\rm calc}, \\ T_{1/2}^{\rm calc}/T_{1/2}^{\rm expt} & \text{if} \quad T_{1/2}^{\rm expt} < T_{1/2}^{\rm calc}. \end{cases} \tag{30}$$

Table VI shows the analysis of the present work and Refs. [8,9]. The numbers given in Table VI(b) are taken from TABLE A of Ref. [8] and TABLE A of Ref. [9]. In the table, N denotes the number of nuclei with experimental half-lives which satisfy the condition shown in the second column, n is the number of nuclei which satisfy the condition in the first column. Generally, the accuracy of our present calculation is slightly worse than in Refs. [8,9]. This can be expected because the present model includes only three parameters, χ_0, κ_0, and μ, which specify the strengths of the ph and pp GT forces, whereas in Refs. [8,9] the strengths are fixed separately for each isotopic chain; this means that the models in Refs. [8,9] have larger degrees of freedom in adjusting the calculation to experimental data. It should be noted, however, that the present calculation reproduces the global systematics (28) much better than Refs. [8,9], as shown in the preceding subsection.

Möller *et al.* [10] use a quite similar pnQRPA model with only the ph GT force, whose strength is inversely proportional to the mass number, namely $\chi_{\rm GT} = 23/A$ MeV. By this parametrization of the ph GT force, the position of the experimental GTGR is reproduced only at ^{208}Pb. Also in their calculations, some individual choices of nuclear parameters were made. They analyze the error of their calculated half-lives by the mean error

$$M_{r_1} = \frac{1}{n}\sum_{i=1}^{n} r_1^i, \quad M_{r_1}^{10} = 10^{M_{r_1}} \tag{31}$$

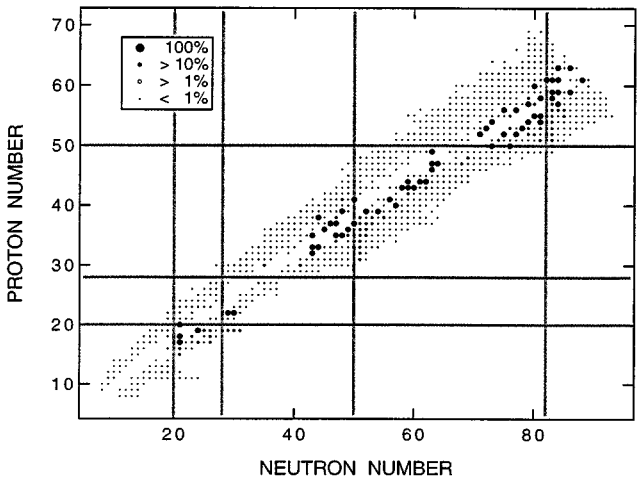

FIG. 9. Contribution of unique first-forbidden transition to total transition probability.

and the spread around the mean

$$\sigma_{r_1}=\left[\frac{1}{n}\sum_{i=1}^{n}(r_1^i-M_{r_1})^2\right]^{1/2}, \quad \sigma_{r_1}^{10}=10^{\sigma_{r_1}}, \tag{32}$$

where

$$r_1=\log_{10}(T_{1/2}^{\rm calc}/T_{1/2}^{\rm expt}). \tag{33}$$

Table VII shows the comparison of the accuracy between the present calculation and the data taken from Ref. [10]. It is seen that the present calculation generally gives better agreement with experiment for both the mean $M_{r_1}^{10}$ and the spread around the mean $\sigma_{r_1}^{10}$. The accuracy of the calculation is improved more for β^+ decay and electron capture than for β^- decay in the present calculation, compared to the result of Ref. [10], probably because of the inclusion of the pp GT interaction which affects significantly the GT strength in β^+ direction.

Finally, Table VIII shows the same analysis separately for nuclei with proton number $Z\leqslant 40$ which are included in the fit of the strengths of the GT forces, and for those which are not included in the fit. The error of the calculated β-decay half-lives are same order for both groups and it is expected that the present model can be safely extrapolated to heavier nuclei and nuclei with large neutron excess which are of interest in astrophysical problems.

C. Effects of forbidden decay

In the calculation presented so far, we have considered only allowed β transitions. The inclusion of forbidden transitions is one possibility to improve the model. Here we introduce a schematic interaction which is relevant to unique first-forbidden transitions, and study its effects on the calculated β-decay half-lives.

The probabilities of the unique first-forbidden (U1F) transitions are obtained in the same way as the Gamow-Teller case described in Sec. II, except that the ph and pp matrix elements are substituted by

$$V_{pn,p'n'}^{\rm ph}=+2\chi_{\rm U1F}f_{pn}(\mu)f_{p'n'}(\mu), \tag{34}$$

$$V_{pn,p'n'}^{\rm pp}=-2\kappa_{\rm U1F}f_{pn}(\mu)f_{p'n'}(\mu). \tag{35}$$

Here

$$f_{pn}(\mu)=\langle p|t_-r[\sigma Y_1]_{2\mu}|n\rangle \tag{36}$$

is a single-particle U1F transition amplitude and now μ takes the values $\mu=0,\pm1$, and ±2, and the proton and neutron states p and n have opposite parities.

TABLE IX. Contribution of unique first-forbidden transition to total β-transition probability for $N=21$ and $N=83$ nuclei. $T_{1/2}^{\rm total}$ is the total half-life including both allowed and unique first-forbidden decay and $T_{1/2}^{\rm allowed}$ is the partial half-life for allowed β decay. The dash indicates that the calculation predicts no allowed transition.

Z	N	Direction	$T_{1/2}^{\rm expt}$ (s)	$T_{1/2}^{\rm allowed}$ (s)	$T_{1/2}^{\rm total}$ (s)	Contribution (%)
15	21	β^-	5.90×10^{0}	1.38×10^{2}	1.36×10^{2}	1.7
16	21	β^-	3.03×10^{2}	1.48×10^{2}	1.46×10^{2}	1.6
17	21	β^-	2.23×10^{3}		4.36×10^{8}	100.0
18	21	β^-	8.49×10^{9}		7.60×10^{9}	100.0
20	21	β^+	3.25×10^{12}		7.40×10^{11}	100.0
50	83	β^-	1.47×10^{0}	5.07×10^{1}	4.50×10^{1}	11.4
51	83	β^-	8.50×10^{-1}	3.71×10^{2}	3.40×10^{2}	8.1
52	83	β^-	1.92×10^{1}	2.89×10^{3}	1.26×10^{3}	56.3
53	83	β^-	8.40×10^{1}	9.57×10^{3}	4.96×10^{3}	48.2
54	83	β^-	2.29×10^{2}	4.51×10^{3}	3.72×10^{3}	17.4
55	83	β^-	1.93×10^{3}	6.83×10^{4}	3.74×10^{4}	45.2
56	83	β^-	5.08×10^{3}	3.74×10^{4}	3.55×10^{4}	5.0
57	83	β^-	1.45×10^{5}	8.79×10^{4}	8.59×10^{4}	2.3
58	83	β^-	2.81×10^{6}		1.31×10^{9}	100.0
59	83	β^-	6.89×10^{4}		9.53×10^{11}	100.0
61	83	β^+	3.14×10^{7}		7.56×10^{10}	100.0

For a preliminary analysis, we adjust the strengths χ_{U1F} and κ_{U1F} to half-lives of several light nuclei which decay through only U1F transitions, assuming a $1/A$ dependence. We obtain the best-fit values,

$$\chi_{\mathrm{U1F}}=5.6/A \text{ MeV fm}^{-2}, \quad \kappa_{\mathrm{U1F}}=0. \tag{37}$$

Figure 9 graphically shows the contribution of U1F transitions to the total transition probability calculated using the above strength parameters. A larger contribution is seen in near-stable and near-magic nuclei, for which the calculation with only allowed transitions is generally inaccurate. Table IX lists some examples for nuclei with neutron number $N=21$ and $N=83$. Good agreement between the calculation and experiment is obtained for ^{39}Ar and ^{41}Ca, for which β-decay is known experimentally to be dominated by $\Delta J^{\pi}=2^{-}$ transitions. Meanwhile, for $N=83$ nuclei the calculation taking only the allowed and U1F transitions into account overestimates β-decay half-lives. This suggests a possibility that $\Delta J^{\pi}=0^{-}$ and 1^{-} transitions also have considerable contributions for those nuclei.

The above analysis shows that forbidden transitions can have large contributions especially for near-magic nuclei. The present study includes only unique forbidden transitions, so it is worthwhile studying effects of non-unique forbidden transitions which are expected, for some nuclei, to have still larger contribution to the calculated half-lives.

V. SUMMARY

We have presented a systematic study of beta-decay properties of nuclei in the pnQRPA model which includes the particle-hole and particle-particle terms of the separable GT residual interaction consistently for both β^{-} and β^{+} directions, assuming that the strengths of the GT forces are smooth functions of mass number A, i.e., proportional to A^{μ} with μ being a constant. The strength of the particle-hole force is determined by adjusting the calculated positions of the GT giant resonance to observed values for ^{48}Ca, ^{90}Zr, and ^{208}Pb. This gives the mass dependence of the strength $\propto 1/A^{0.7}$, which is different from the previously accepted $1/A$ dependence [13,14]. The same mass dependence is assumed for the strength of the particle-particle force, and the coefficient is determined by a least-squares-fit to observed β-decay half-lives of nuclei with $Z\leqslant 40$. We also propose the use of averaged properties between the parent and daughter nuclei for the model parameters in the Nilsson+BCS calculation, and show that this choice is in fact valid for a reliable prediction of β-decay half-lives.

The fixed parameters are used to calculate β-decay half-lives of nuclei up to $A=150$. The calculation is generally in good agreement with experiment, and no significant changes in accuracy of the calculated half-lives are found for heavier nuclei, in comparison with nuclei with $Z\leqslant 40$. The prediction is more accurate for nuclei with shorter half-lives, and the calculation reproduces 97% of the experimentally known half-lives shorter than 1 s within a factor of 10. It is also confirmed that the calculated half-lives well satisfy the semi-empirical inequalities [22], probably because of the smooth variations of the strengths of the GT forces. It is thus expected that the parameters used in the present calculation are also valid for nuclei with large neutron excess, which are of interest in astrophysical problems.

The calculated half-lives are relatively inaccurate for near-stable and near-magic nuclei. We have shown, for some of those nuclei, that the unique first-forbidden transition has large contribution and its inclusion greatly improves the calculated half-lives. This suggests that the inclusion of nonunique forbidden transitions is also effective to improve the model. Besides the inclusion of forbidden transitions, refinements in the underlying single-particle and pairing models [13] may also improve the calculation.

In spite of many possibilities of refinements, the present pnQRPA model is expected to give useful results concerning nuclear β-decay properties needed for resolving astrophysical problems. Especially, it can be used to calculate weak interaction rates of nuclei at high temperature and high density, which are of decisive importance in a study of the stellar evolution, and we hope to do this in the future. Now we are preparing to apply the present model to nuclei throughout the periodic system, up to the proton and neutron drip lines, aiming at a unified understanding of nuclear β-decay properties. We plan to publish the table of β-decay half-lives when we have finished the calculation for all nuclei.

ACKNOWLEDGMENTS

This work was financially supported in part by a Grant-in-Aid for Cooperative Research (05243204, 06234206) from the Ministry of Education, Science and Culture, and by Research Center for Nuclear Physics, Osaka University, as RCNP Computational Nuclear Physics Project (Project No. 94–B–02). Numerical calculations were performed with the FACOM M780 and VP2100 computer systems at Institute for Nuclear Study, University of Tokyo, and with the HITAC M-880 computer system at the Computer Center of University of Tokyo.

[1] B. H. Wildenthal, Prog. Part. Nucl. Phys. **11**, 5 (1984).
[2] B. A. Brown and B. H. Wildenthal, At. Data Nucl. Data Tables **33**, 347 (1985).
[3] M. Hino, K. Muto, and T. Oda, Phys. Rev. C **37**, 1328 (1988).
[4] K. Muto, E. Bender, and T. Oda, Phys. Rev. C **43**, 1487 (1991).
[5] M. Takahara, M. Hino, T. Oda, K. Muto, A. A. Wolters, P. W. M. Glaudemans, and K. Sato, Nucl. Phys. **A504**, 167 (1989).
[6] T. Oda, M. Hino, K. Muto, M. Takahara, and K. Sato, At. Data Nucl. Data Tables **56**, 231 (1994).
[7] K. Takahashi and M. Yamada, Prog. Theor. Phys. **41**, 1470 (1969).
[8] A. Staudt, E. Bender, K. Muto, and H. V. Klapdor-Kleingrothaus, At. Data Nucl. Data Tables **44**, 132 (1990).
[9] M. Hirsch, A. Staudt, K. Muto, and H. V. Klapdor-Kleingrothaus, At. Data Nucl. Data Tables **53**, 165 (1993).

[10] P. Möller, J. R. Nix, and K.-L. Kratz, At. Data Nucl. Data Tables (to be published).
[11] J. A. Halbleib and R. A. Sorensen, Nucl. Phys. **A98**, 542 (1967).
[12] J. Randrup, Nucl. Phys. **A207**, 209 (1973).
[13] P. Möller and J. Randrup, Nucl. Phys. **A514**, 1 (1990).
[14] E. Bender, K. Muto, and H. V. Klapdor, Phys. Lett. **B208**, 53 (1988).
[15] K. Muto, E. Bender, and H. V. Klapdor, Z. Phys. **A333**, 125 (1989).
[16] K. Muto, E. Bender, T. Oda, and H. V. Klapdor-Kleingrothaus, Z. Phys. A **341**, 407 (1992).
[17] D. Cha, Phys. Rev. C **27**, 2269 (1983).
[18] J. Engel, P. Vogel, and M. R. Zirnbauer, Phys. Rev. C **37**, 731 (1988).
[19] K. Muto, E. Bender, and H. V. Klapdor, Z. Phys. A **334**, 47 (1989).
[20] V. A. Kuz'min and V. G. Soloviev, Nucl. Phys. **A486**, 118 (1988).
[21] M. Yamada and T. Tachibana, in *Proceedings of the International Symposium on Origin and Evolution of the Elements, Tokyo, 1992*, edited by S. Kubono and T. Kajino (World Scientific, Singapore, 1992), p. 234.
[22] T. Kondoh and M. Yamada, Prog. Theor. Phys. Suppl. **60**, 136 (1976).
[23] P. Möller, J. R. Nix, W. D. Myers, and W. J. Swiatecki, At. Data Nucl. Data Tables **59**, 185 (1995).
[24] The Particle Data Group, Phys. Lett. B **204**, 1 (1988).
[25] N. B. Gove and M. J. Martin, Nucl. Data Tables **10**, 205 (1971).
[26] M. J. Martin and P. H. Blichert-Toft, Nucl. Data Tables **A8**, 1 (1970).
[27] E. Browne, J. M. Dairiki, and R. E. Doebler, in *Table of Isotopes, seventh edition*, edited by C. M. Lederer and V. S. Shirley (Wiley, New York, 1978).
[28] S. G. Nilsson, Mat. Fys. Medd. Dan. Vid. Selsk. **29**, No. 16 (1955).
[29] I. Ragnarsson and R. K. Sheline, Phys. Scr. **29**, 385 (1984).
[30] J. Blomqvist and A. Molinari, Nucl. Phys. **A106**, 545 (1968).
[31] A. Bohr and B. R. Mottelson, *Nuclear Structure* (Benjamin, New York, 1969), Vol. I.
[32] E. Bender, Diplomarbeit, Max-Planck-Institut für Kernphysik, 1988.
[33] P. Möller and J. R. Nix, At. Data Nucl. Data Tables **39**, 213 (1988).
[34] E. Browne and R. B. Firestone, in *Table of Radioactive Isotopes*, edited by V. S. Shirley (Wiley, New York, 1986).
[35] G. Audi and A. H. Wapstra, Nucl. Phys. **A565**, 1 (1993).
[36] C. Gaarde, J. S. Larsen, C. D. Goodman, C. C. Foster, C. A. Goulding, D. J. Horen, T. Masterson, J. Rapaport, T. N. Taddeucci, and E. Sugarbaker, *Proceedings of 4th International Conference on Nuclei Far from Stability, Helsingør, 1981* (CERN 81-09, Geneva, 1981), p. 281.